ELSEVIER

Journal of Alloys and Compounds 452 (2008) 336–342

Journal of ALLOYS AND COMPOUNDS

www.elsevier.com/locate/jallcom

Characterization and properties of nanocrystalline surface layer in Mg alloy induced by surface mechanical attrition treatment

Ying-hui Wei [a,*], Bao-sheng Liu [a], Li-feng Hou [a], Bing-she Xu [a], Gang Liu [b]

[a] *College of Materials Science and Engineering, Taiyuan University of Technology, Taiyuan 030024, PR China*
[b] *Shenyang National Laboratory for Materials Science, Institute of Metal Research, Chinese Academy of Sciences, Shenyang 110016, PR China*

Received 1 October 2006; received in revised form 9 November 2006; accepted 9 November 2006
Available online 3 January 2007

Abstract

By means of surface mechanical attrition treatment (SMAT), a nanocrystalline (NC) surface layer about 40 μm was synthesized on an AZ91D Mg alloy. The microstructural features of the surface layer produced by SMAT were systematically characterized by optical microscopy (OM) observations, X-ray diffraction (XRD), transmission electron microscopy (TEM) and high-resolution transmission electron microscopy (HRTEM) investigations, and hardness measurement was also carried out in order to examine the hardness variation along the depth. Experimental results show that the microstructure is inhomogeneous along the depth. In the region from top surface to about 10 μm in depth, the grain size increases from about 50 nm to 100 nm. In the adjacent region of about 10–40 μm in depth, the grain size increases from about 100 nm to 400 nm. The grain refinement can be attributed to the activity of dislocation and occurrence of dynamic recrystallization. Moreover, emergence of stacking faults in the grain interior is a novel discovery. After the SMAT, the micro-hardness of the surface layer was enhanced significantly compared with that of the original sample.

Keywords: Metals; Surface mechanical attrition treatment; Surface nanocrystallization; Dynamic recrystallization; Micro-hardness

1. Introduction

It has been over 20 years since Herbert Gleiter first presented the concepts for developing nanocrystalline (NC) materials (that is, ultra-fine grained materials with a grain size less than 100 nm) with special properties [1]. Since then, the field of NC materials has developed rapidly, owing to tremendous interest in this topic of scientific and technological importance. Meanwhile, a variety of synthesis techniques have been developed for producing bulk NC materials, e.g. the crystallization of amorphous precursors [2], electro-deposition [3] and severe plastic deformation of bulk materials [4].

The resultant fine grain microstructures provide a significant increase in both the low and high temperature strength and the tribological properties. However, there are still two major obstacles for development of bulk NC materials. First, it is difficult to manufacture of porosity-free and contamination-free samples. Second most of the current techniques for synthesizing bulk NC materials are not adapted to be produced on an industrial scale due to limitations in terms of sample size and cost.

In fact, the majority of failures modes of engineering materials, such as fatigue fracture, fretting fatigue, wear and corrosion, etc., are very sensitive to the microstructures and properties of the materials surface, and in most cases materials failures occurred on the surface. Therefore, optimization of the surface microstructures of materials may effectively enhance the combination performance in service of the materials. Surface mechanical attrition treatment (SMAT) [5] cannot only form the nanostructure of porosity-free and contamination-free on materials surface layer, but also avoid bonding interface between the NC surface layer and matrix. If SMAT process is combined with other surface techniques, it would be expected to strengthen material surface, to avoid service failure and to prolong service time.

The investigation of SMAT is underway. Lu et al. have studied elementarily the process engineering, nanostructure formation mechanism and material properties after SMAT for various

* Corresponding author. Tel.: +86 351 6018683; fax: +86 351 6010311.
E-mail address: yhwei@public.ty.sx.cn (Y.-h. Wei).

0925-8388/$ – see front matter © 2006 Elsevier B.V. All rights reserved.
doi:10.1016/j.jallcom.2006.11.079

materials, such as stainless steel [6,7], pure Fe [8], Al alloy [9] and so on, and acquired some guided production. However, at present, the materials investigated after SMAT are limited, which are of face-centered cubic (fcc) or body-centered cubic (bcc) systems. And many basal scientific issues are still unclear, especially deformation mechanism of materials and grain refinement mechanism under various strain rates.

So far, most documented experimental and theoretical investigations in the literatures showed that the grain refinement is originated from dislocation activities during deformation in cubic metals and alloys with a medium to high stacking fault energy (SFE). Plastic straining generates high density dislocations arranged into various configurations depending on the nature of materials, such as the geometrically necessary boundary, incidental dislocation boundary, and dense dislocation wall, etc. [8,10]. These dislocation boundaries increase their disorientations with increasing strain, and some of them will become high angle ones, which subdivide the original grains down to refined grains. In contrast, the low SFE fcc materials exhibit a different mode of grain refinement. In an Inconel 600 alloy [11] and stainless steel [6,7] (both have low SFEs), for example, the grain refinement involves the dislocations slip and subsequent deformation twinning, followed by interplay of twins with dislocations. For the hexagonal close packed (hcp) metals, the deformation twinning occurs at the early stage of deformation and serves as an additional deformation mechanism to dislocation slip in order to satisfy the von Mises criterion [12]. The transition of strain accommodation from twinning to dislocation slip with increasing strain is responsible for the grain refinement in titanium [13] during the process of SMAT.

In present work, the most attractive AZ91D Mg alloy with superior specific stiffness and strength was chosen for SMAT in order to explore both the formation mechanism of nanocrystallization and characterization of deformation layer. It was proved that the dislocations and dynamic recrystallization are the main deformation mechanism. Stacking faults (SFs) were found firstly in the interior of the many nanograins.

2. Experimental methods

2.1. Materials

The material used in the experiment is cast AZ91D Mg alloy. The specimen for SMAT is 100 mm × 100 mm × 10 mm in dimensions and is cut from the commercial Mg alloy ingot. The chemical composition of the material is given in Table 1. The microstructures of the AZ91D Mg alloy consist of α-Mg (hexagonal crystal structure, $a = 0.32094$ and $c = 0.52105$ nm) grains together with intergranular β-$Mg_{17}Al_{12}$ (cubic crystal structure, $a = 1.056$ nm) grains [14]. The β-phase is about 15.4 wt% at this AZ91D Mg alloy. The average grain size of α-Mg is about 100 μm. Before SMAT, the sample surfaces were polished with 600-grate SiC papers.

Table 1
Chemical composition of the AZ91D magnesium alloy investigated

Al	Zn	Mn	Si	Fe	Ni	Cu	Be	Mg
8.63	0.66	0.29	0.032	0.0014	<0.0005	0.0025	0.0006	Balance

2.2. SMAT

SMAT was performed in vacuum using a SNC-1 machine. The detail description of this apparatus was reported previously [15]. GCr15 steel balls of 6 mm in diameter were placed at the bottom of a cylinder-shaped vacuum chamber that was vibrated by a generator, with which the balls were resonated. Because of the high vibration frequency of the system (50 Hz in the experiment, which can be varied up to 20 kHz), the sample surface to be treated was peened by a large number of balls in a short period of time. Each peening of the ball to the surface would result in plastic deformation on the surface layer of the treated sample. As a consequence, repeated multidirectional peening at high strain rates onto the sample surface lead to severe plastic deformation on the specimens' surface layer.

The average surface roughness (R_a) of AZ91D Mg alloy samples before and after SMAT are 0.42, 1.37 (treated for 10 min) and 1.39 μm (treated for 30 min), respectively. The comparable R_a values indicate the surface roughness has been increased slightly after the SMAT, and the values would not change with treated time.

2.3. Microstructural examinations

An Axiovert25CA (zeiss) optical microscope was used to examine the microstructural development along sections perpendicular to the treated surface of the specimen. The microstructures of the sample surface were studied by X-ray diffraction (XRD) with Cu target radiation in a Rigaku D/max-2400 X-ray diffract meter. The average grain size was obtained from XRD line broadening. The microstructures were observed in a transmission electron microscopy (TEM H-800) and high-resolution TEM (JEOL-2010) operating at 200 kV. The plane-view TEM foil of deformation layer was obtained first by polishing the sample mechanically on the untreated side until it was about 30 μm thick; followed by Ar ion milling using a Gatan Precision Ion Polishing System (PIPS) with a small incident angle (5°) and the vacuum degree of 7.6×10^{-3} Pa, allowing large, thin and homogeneous areas to be observed. A Leco M-400-H1 hardness tester was used to examine the micro-hardness of the specimen. The surface roughness (R_a) of AZ91D Mg alloy samples was measured by 2205 A measuring apparatus.

3. Results and discussion

3.1. Microstructures of surface layer

The cross-sectional OM observation of the SMATed AZ91D Mg alloy sample for 30 min is shown Fig. 1. Microstructure morphology of the as-treated surface layer (of about 40 μm in thick) differs obviously from that in the matrix. The evidences of severe plastic deformation can be seen in the surface layer. Grain boundaries and β-phase ($Mg_{17}Al_{12}$) could not be identified in OM observation as well as in the matrix.

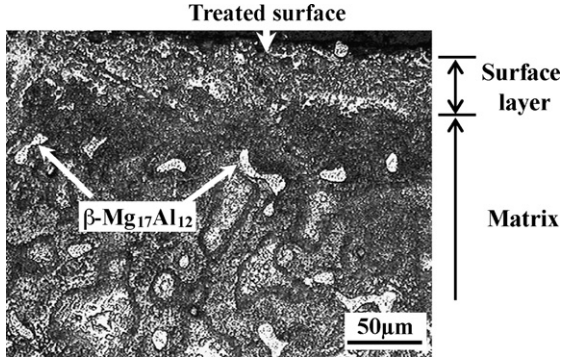

Fig. 1. Cross-sectional optical micrographs closed to the SMATed surfaces, treated for 30 min.

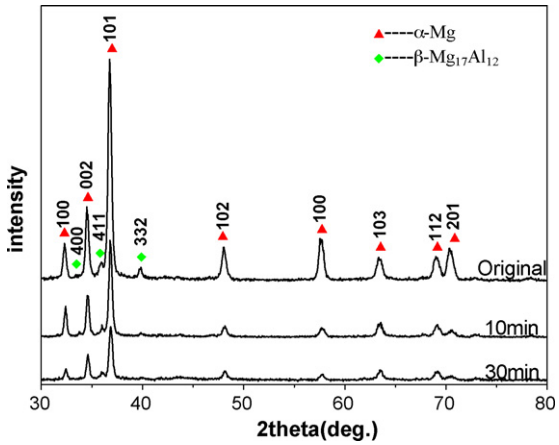

Fig. 2. XRD patterns of the AZ91D magnesium alloy sample before and after SMAT for different times (original, 10 min and 30 min).

The XRD patterns of AZ91D Mg alloy samples before and after SMAT are shown in Fig. 2. It is observed that after SMAT, there are an evident broadening of the Bragg reflections and a slight shift in the centroid position of diffraction peaks relative to the coarse-grained sample. This might be attributed to grain refinement, microstrain development and micro-distortions of the crystalline lattice. This phenomenon is common in many SMATed materials. The average grain size of the surface layer after SMAT was calculated to be 62 ± 4 nm when treated for 10 min. With a prolonged treating time (30 min), the average grain size reduced to 51 ± 2 nm. These realities suggested that the average grain size of the top surface layer (from the top surface to the depth of 5 μm) reduced with treating time.

Based on the optical micrograph of specimen SMATed for 30 min, depths of about 10, 30–40 and 50–60 μm from the SMATed surface were selected for TEM investigation.

TEM micrographs in Fig. 3 show the deformation feature in the area closed to the free strain matrix (50–60 μm depth from the top surface). This area corresponds to the initial stage of plastic deformation. A large number of dislocation walls (DWs) and dislocation tangles (DTs) (indicted by two black arrowheads in Fig. 3a) are found in the subgrains interior, responsible for the work-hardening during dynamic straining. DWs may transform to individual subgrains depending upon further plastic straining. In fact, the evidence of subgrains (indicted by a white arrowhead in Fig. 3b) at triple grain junctions has been observed. It is reasonable to believe the DWs and DTs are the main cause of the subdivision of subgrains and the formation of NC with the increasing strain. It has also been observed that the dislocation density is often lower near subgrains than it is in the other grains (Fig. 3a). The microstructural observations indicate that additional strain accommodation is achieved by successive grain subdivision.

It is well known that the deformation modes (twinning, slip) have a considerable influence on the mechanism of grain refinement. In Al (fcc) and Fe (bcc), for instance, dislocation slip is the main deformation mode and it has been found to dominate the grain subdivision process down to the nanometer scale when SMAT is carried out [8,9]. In other metals such as stainless steel, dislocation slip is the prevalent deformation mechanism at low strain and is converted into twinning as the strain increases [6,7]. On the contrary, among the majority of HCP metals, such as titanium, twinning is the customary deformation mode at low strain, and then it is taken over by dislocation slip as the strain increases [13]. However, in present study of AZ91D Mg alloy, no twinning was found at initial stage of plastic deformation.

Fig. 4 shows the microstructures (about 30 μm in depth from the top surface) where the grains size are 300–400 nm. Selected area electron diffraction (SAED) patterns exhibit well-defined rings than they are in Fig. 3c, which show that the nanograins are disoriented. In this area, the grains size is smaller than it is in the low strain area closed to the matrix, indicating the grains are fine-cut as the strain increases.

Fig. 5 shows the TEM micrographs of the surface layer (about 10 μm thick) of the sample after SMAT, (a) bright-field image and (b) Dark-field image showing equiaxed nanograins. From the dark field image (Fig. 5b), one can see nanoscale grains, which are roughly equiaxed in shape. The corresponding SAED

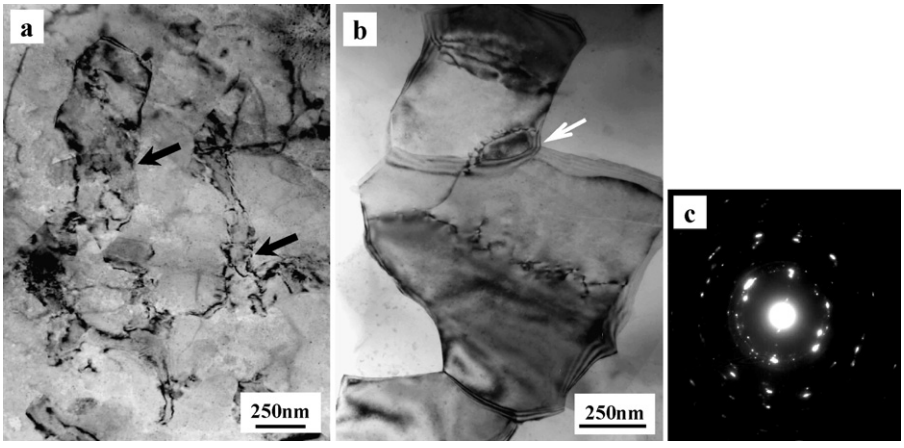

Fig. 3. TEM micrographs show deformation feature in the area closed to the free strain matrix (50–60 μm in depth from the top surface). (a) Bright field image shows dislocation walls and dislocation inside the interior of submicronic polygonal grains (indicted by a pair of black arrowhead); (b) bright field image of dislocation pile-ups and subgrains (indicted by a white arrowhead) on grain boundaries; (c) corresponding SAED pattern of (a).

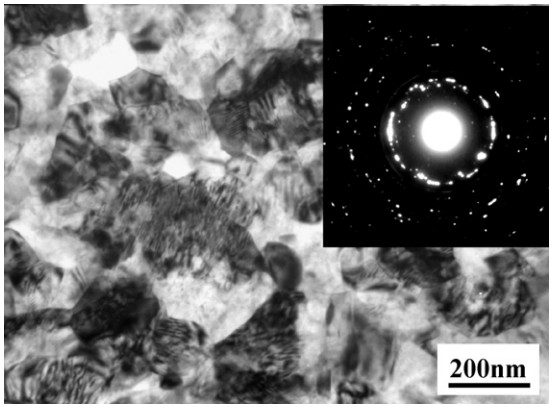

Fig. 4. Bright field image and corresponding SAED pattern of 40 μm in depth from the top surface.

patterns (Fig. 5c) exhibit more entire rings than those at a depth of about 30 μm (Fig. 4), which illustrates the formation of finer grains with a more random orientation on the treated surface. The average grain size at the depth of about 10 μm is approximate 100 nm.

Fig. 6a shows the bright-field TEM image of a nanograin. The grain size is about 110 nm in diameter and there exist slather stacking faults in the nanograin interior. The enlarged stacking faults in this grain are indicated by a pair of white arrows in the HRTEM image of Fig. 6b (showing the rectangular area marked in Fig. 6a). Such stacking faults have been observed in a number of nanograins. Some of these stacking faults do not pass across the whole grain, but stop in the grain interior with Shockley partial dislocations located at the front boundaries of the stacking faults. Similar stacking faults are also observed in NC copper deformation via high-pressure torsion [16] and NC Ni under uniaxial tensile deformation [17]. This indicated that these stacking faults nucleated heterogeneously at the grain boundary (GB) and grew into the grain interior via partial dislocation emission from the GB [16]. Simultaneously, Van Swygenhoven et al. [18] and Yamakov et al. [19] showed that the formation of stacking faults involves the partial dislocation activity and hence, would have a significant effect on deformation behavior especially at the nanometer scale.

Five independent slip systems are necessary for polycrystalline materials to undergo homogeneous plastic deformation [12]. Because the Poisson's ratio $c/a = 1.623$ of Mg is almost equal to ideal $c/a = \sqrt{3}$, only four independent slip systems (basal plane $(0\,0\,0\,1)$ and prism plane $(1\,0\,\bar{1}\,0)$) are available in Mg and its alloys, and twinning is essential in order to maintain the necessary deformation capability. However, in present study of AZ91D Mg alloy, no twinning was found. In fact, the twinning deformation was frequently found in pure Mg and some Mg alloys with lower Al content [20,21] when they were subjected to plastic deformation. We thought, hypothetically, the difference of deformation mode among pure Mg, Mg alloys with lower Al content and present AZ91D Mg alloy was due to the Al content. It was well accepted that the addition of alloying agent to other metals and/or alloys would influence their SFEs. The addition of Al often increases their SFE. Zhang and Appel [22] have pointed out that the SFEs decreased significantly with the decrease of Al content, from 97 mJ m^{-2} for 49.6 wt.% Al to 67 mJ m^{-2} for 48 wt.% Al in the binary TiAl alloy. In other words, the SFEs of the binary TiAl alloy would increase significantly with the increasing Al content. Oh et al. [23] and Han and Hong [24] have also showed, in Fe–Mn–Cr–Al–C alloy system, the SFEs increased with increasing Al content. The addition of Al, nevertheless, did not increase the SFEs of all alloy systems. For instance, the SFEs decreased with increasing Al content, in Cu and Ag alloys system, until Al content added up to 40 at.% [25]. Fortunately, preceding hypothesis is supported by literature [25], which concluded the SFEs increase linearly in the Al–Mg system when adding of Al to Mg.

Owing to the structural characteristics of nanograins described above, it is assumed that a recrystallization process may play an important role in their formation. That recrystallization can be considered as dynamic since it occurs during the SMAT process. Derby [26] has ever carried out a systematic analysis of dynamic recrystallization in relation to two mechanisms: nucleation and the growth of recrystallized grains in a deformed material (classical recrystallization) and the formation of recrystallization by the gradual rotation of subgrains (rotation recrystallization). Both mechanisms lead to the break-up of the original grain structure. In classical or migration recrystalliza-

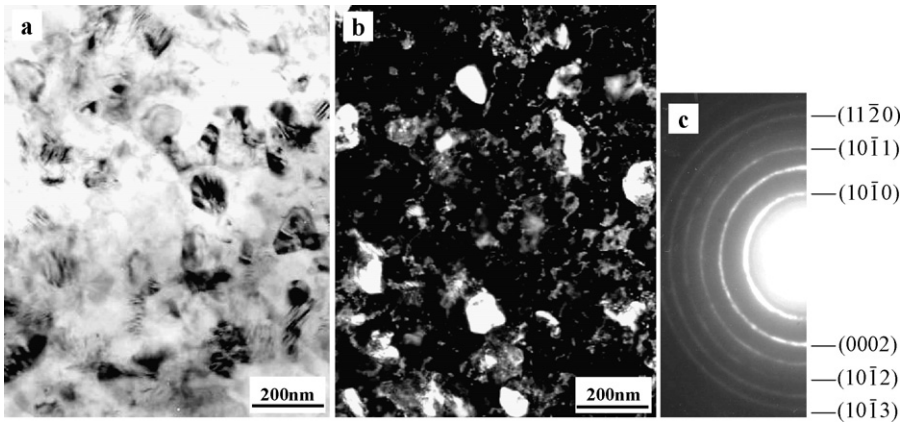

Fig. 5. The TEM micrographs of the surface layer (about 10 μm thick) of the SMATed sample for 30 min, (a) bright-field image and (b) dark-field image shows equiaxed nanograins; (c) corresponding SAED pattern of (b).

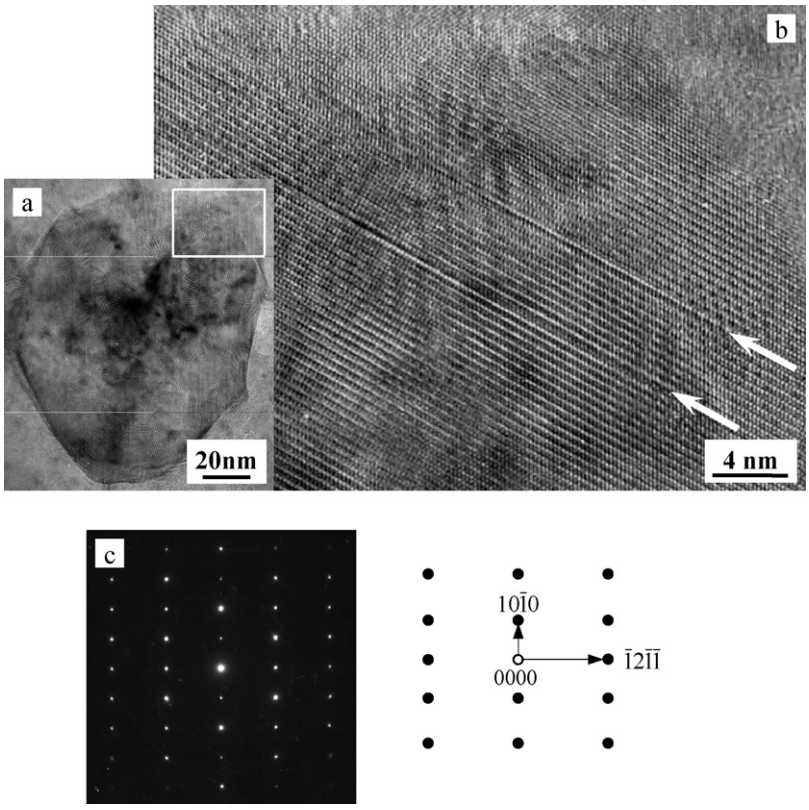

Fig. 6. A bright-field image shows a nanograin (a), the HRTEM micrograph shows the presence of SFs marked by a pair of white arrowheads (b), and SAED pattern corresponded (a).

tion, new grains are nucleated in areas of high plastic strain and grow into the deformed material. In rotation recrystallization, rotation of the cells and subgrains occurs gradually until all the dislocations are absorbed by the grain boundaries.

In general, nucleation and growth of recrystallized nuclei occur as a result of hot deformation. Under severe plastic deformation conditions, such as torsional straining, the recrystallization temperature is reduced. A very high strain and strain rate are also produced during the SMAT process and a certain amount of adiabatic heating may occur but it is difficult to evaluate the exact temperature of the top treated surface. Also, TEM examinations do not show evidence of nucleation and growth mechanism for nanograins but indicate clearly the importance of grain boundary rotation in microstructural development. It is, therefore, suggested that rotation recrystallization may play a major role in the final grain refinement mechanism during SMAT. Actually, Ion et al. [27] showed that dynamic recrystallization in Mg is attributed to the constraint imposed by the lack of easily activated slip systems rather than to the effect of SFEs at the process of deformation. According to their results, the formation of new grains in the Mg alloy results from severely rotated regions adjacent to grain boundaries. This type of dynamic recrystallization is termed rotation recrystallization.

In terms of XRD analysis, as well as OM and TEM observations, the variation of the grain size of AZ91D Mg alloy along the depth was determined, as shown in Fig. 7. Differences exist in results between TEM observations and XRD analysis, owing to different measurement principles [9]. The grain size in the surface layer increases with the increasing depth. The surface layer can be subdivided into two sections along the depth from the top treated surface based on the variation of microstructure: (i) a nanostructured region (0–10 μm deep) and (ii) a submicro-sized and micro-sized region with evident plastic deformation (about 10–40 μm deep).

3.2. Hardness

The variation of micro-hardness along depth of SMA Mg alloy treated for 30 min was depicted in Fig. 8. The micro-

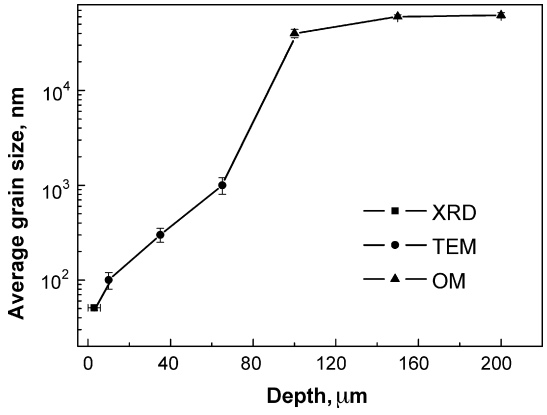

Fig. 7. Variation of the grain size with the depth from the top treated surface in the SMATed sample, determined by means of TEM and OM observations, XRD analysis.

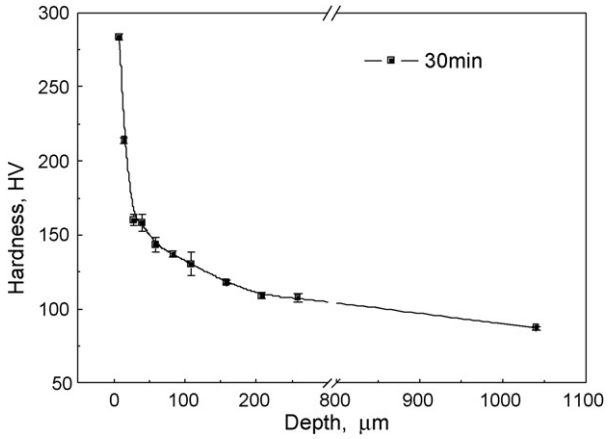

Fig. 8. Hardness evolution along the depth of the SMATed sample for 30 min.

hardness of the top surface layer (consisting NC grains) is three times more than that of the matrix. The increment of micro-hardness may be associated with two main factors. Firstly, the increase of micro-hardness may be attributed to grains refinement on the surface layer following the classical Hall–Petch relationship [28,29]. According to Hall–Petch equation:

$$\sigma = \sigma_0 + Kd^{-1/2} \quad (1)$$

where σ is the yield stress, σ_0 the yield stress of a single crystal, K a constant and d is the grain size. The value of K increases with increasing the Taylor factor [30]. The relationship is also similarly applicable for hardness. The Taylor factor generally depends upon the number of the slip systems. Because the slip systems are limited and the Taylor factor is larger for hcp metals than that for fcc and bcc metals, the hcp metals exhibit the strong influence of the grain size on strength. It is, therefore, suggested that high strength can be attained in fine-grained Mg-based materials. Secondly, the enhancement of micro-hardness is probably attributed to the re-dissolution of β-phase, as shown in Fig. 1 and Fig. 2. No β-phase can be found on the treated surface layer. The dissolution of β-phase and the solution of Al in Mg alloy have been simultaneously induced by the increased strain. In general, the microstructure of the cast Mg alloy consists of α-Mg and β-$Mg_{17}Al_{12}$, which is stable at room temperature. Subjecting to SMAT, the refined α-Mg and β-$Mg_{17}Al_{12}$ in same depth in the specimen treated are almost simultaneously induced. It is not difficult to comprehend the increase of the grain boundaries in quantity and distortion of lattice relative to original coarse grains, which give rise to increased interface free energy and strain energy. It is well accepted that a system has the tendency of spontaneous transforming to lower Gibbs free energy state. Thus, any events (such as the re-dissolution of β-phase) reducing Gibbs free energy of the system considered may take place. The driving force of re-dissolution of the β-phase is mainly composed of increased interface free energy and strain energy between α-Mg and the β-phase refined by SMAT. And also, the interface misfit of the two phases, due to the difference of lattice types, hcp and bcc respectively, and deformation mechanisms, is an important factor to promote the β-phase re-dissolution. In addition, from a kinetic point of view, the re-dissolution of the β-phase is also greatly advantageous. The defects, severe distortion of lattice and stored strain energy, during the SMAT process, are all helpful for the solute diffusion [31]. The re-dissolution of β-phase is helpful for the increase of micro-hardness, according to present experiment, but its effect on other properties still needed to be investigated continually.

4. Conclusions

NC surface layer was successfully synthesized on an AZ91D Mg alloy by SMAT. The microstructure is inhomogeneous along the depth. In the region from top surface to about 10 μm depth, the grain size increases from about 50 nm to 100 nm. In the adjacent region of about 10–40 μm depth the grain size increases from about 100 nm to 400 nm. The grain refinement behaviors can be associated with the activity of dislocation and occurrence of dynamic recrystallization. Moreover, emergence of stacking faults in the grain interior is first observed. After the SMAT, the micro-hardness of the surface layer is enhanced significantly compared with that of the original sample, which may be attributed to the refinement of grains and the re-dissolution of β-phase in the surface layer. This work demonstrates that the microstructure and the properties of the material surface can be optimized by generating a NC surface layer by means of SMAT.

Acknowledgements

The authors gratefully acknowledge the National Natural Science Foundation (50471070), PR China, the Natural Science Foundation (20041023, 20051050), and the Young Subject-Leader foundation, Shan xi Province for funding provided in support of this work. Financial supporting from NCET-04-0257 is also appreciated.

References

[1] R. Birringer, H. Gleiter, H.P. Klein, P. Marquqrdt, Phys. Lett. A 102 (1984) 365–369.
[2] K. Lu, J.T. Wang, W.D. Wei, J. Appl. Phys. 69 (1991) 522–524.
[3] U. Erb, A.M. El-Sherik, G. Palumbo, K.T. Aust, Nanostruct. Mater. 2 (1993) 383–390.
[4] R.Z. Valiev, A.V. Korznikov, R.R. Mulyukov, Mater. Sci. Eng. A 168 (1993) 141–148.
[5] K. Lu, J. Lu, J. Mater. Sci. Technol. 15 (1999) 193–197.
[6] H.W. Zhang, Z.K. Hei, G. Liu, J. Lu, K. Lu, Acta Mater. 51 (2003) 1871–1881.
[7] G. Liu, J. Lu, K. Lu, Mater. Sci. Eng. A 286 (2000) 91–95.
[8] X. Wu, N. Tao, Y. Hong, B. Xu, J. Lu, K. Lu, Acta Mater. 50 (2002) 2075–2084.
[9] N.R. Tao, Z.B. Wang, W.P. Tong, M.L. Sui, J. Lu, K. Lu, Acta Mater. 50 (2002) 4603–4616.
[10] J.Y. Huang, Y.T. Zhu, H. Jiang, T.C. Lowe, Acta Mater. 49 (2001) 1497–1505.
[11] N.R. Tao, X. Wu, M.L. Sui, J. Lu, K. Lu, J. Mater. Res. 19 (2004) 1623–1629.
[12] Von. Mises, Z. Angew, Math. Mech. 8 (1928) 161.
[13] K.Y. Zhu, A. Vassel, F. Brisset, K. Lu, J. Lu, Acta Mater. 52 (2004) 4101–4110.
[14] R.M. Wang, A. Eliezer, E.M. Gutman, Mater. Sci. Eng. A 355 (2003) 201–207.
[15] K. Lu, J. Lu, Mater. Sci. Eng. A 375–377 (2004) 38–45.

[16] X.Z. Liao, Y.H. Zhao, S.G. Srinivasan, Y.T. Zhu, Appl. Phys. Lett. 84 (2004) 592–594.
[17] X. Wu, Y.T. Zhu, M.W. Chen, E. Ma, Scripta Mater. 54 (2006) 1685–1690.
[18] H. van Swygenhoven, P.M. Derlet, A. Hasnaoui, Phys. Rev. B 66 (2002) 024101.
[19] V. Yamakov, D. Wolf, S.R. Phillpot, A.K. Mukherjee, H. Gleiter, Nat. Mater. 1 (2002) 45–49.
[20] D.L. Yin, K.F. Zhang, G.F. Wang, W.B. Han, Mater. Sci. Eng. A 392 (2005) 320–325.
[21] M.R. Barnetta, M.D. Navea, C.J. Bettles, Mater. Sci. Eng. A 386 (2004) 205–211.
[22] W.J. Zhang, F. Appel, Mater. Sci. Eng. A 329–331 (2002) 649–652.
[23] B.W. Oh, S.J. Cho, Y.G. Kim, et al., Mater. Sci. Eng. 197 (1995) 147–156.
[24] Y.S. Han, S.H. Hong, Mater. Sci. Eng. A 222 (1997) 76–83.
[25] T.C. Schulthess, P.E.A. Turchi, A. Gonis, T.-G. Nieh, Acta Mater. 46 (1998) 2215–2221.
[26] B. Derby, Acta Metall. Mater. 39 (1991) 955–962.
[27] S.E. Ion, F.J. Humphreys, S.H. White, Acta Metall. 30 (1982) 1909–1919.
[28] Z.B. Wang, N.R. Tao, S. Li, et al., Mater. Sci. Eng. A 352 (2003) 144–149.
[29] Z.N. Farhat, Y. Ding, D.O. Northwood, A.T. Alpas, Mater. Sci. Eng. A 206 (1996) 302–313.
[30] R. Armstrong, I. Codd, R.M. Douthwaite, N.J. Petch, Philos. Mag. 7 (1962) 1079.
[31] W.P. Tong, N.R. Tao, Z.B. Wang, J. Lu, K. Lu, Science 299 (2003) 686–688.